

Circular scans for CMB anisotropy observation and analysis

J. Delabrouille,^{1,2} K.M. Górski^{3,4} and E. Hivon³

May 1, 2018

¹ Institut d'Astrophysique Spatiale, CNRS & Université Paris XI, bât 121, 91405 Orsay Cedex, France

² Enrico Fermi Institute, University of Chicago, 5460 South Ellis Avenue, Chicago, IL 60510, USA

³ Theoretical Astrophysics Center, Juliane Maries Vej 30, DK-2100, Copenhagen, Denmark

⁴ On leave from Warsaw University Observatory, Warsaw, Poland

Abstract

A number of experiments for measuring anisotropies of the Cosmic Microwave Background use scanning strategies in which temperature fluctuations are measured along circular scans on the sky. It is possible, from a large number of such intersecting circular scans, to build two-dimensional sky maps for subsequent analysis. However, since instrumental effects — especially the excess low-frequency $1/f$ noise — project onto such two-dimensional maps in a non-trivial way, we discuss the analysis approach which focuses on information contained in the individual circular scans. This natural way of looking at CMB data from experiments scanning on the circles combines the advantages of elegant simplicity of Fourier series for the computation of statistics useful for constraining cosmological scenarios, and superior efficiency in analysing and quantifying most of the crucial instrumental effects.

1 Introduction

The exploration of Cosmic Microwave Background (CMB) is undergoing a boom in both theoretical and experimental directions. The planning of two ambitious space missions, MAP and PLANCK, to be launched in the beginning of the XXI-st century, is one of the sources of stimulus for research in this field. In addition, several long duration balloon-borne experiments are scheduled for operation within the next few years time.

Many of the future CMB anisotropy experiments will perform circular scans on the sky. MAP¹, PLANCK² (Bersanelli et al., 1996), and the balloon-borne experiments TopHat³ and BEAST (Lubin, private communication), will collect data from a large number of intersecting circles, which will then be merged into two-dimensional sky maps. Smaller ground-based experiments as DIABOLO (Benoît et al., in preparation) may scan on only a few circles. In winter 1997 for instance, a one-ring observation of anisotropies was done at the POM2 telescope in the french alps with the DIABOLO instrument.

A common problem in the analysis of the data obtained by performing one dimensional sky scans is that all instrumental effects (other than smoothing by the beam) occur in the monotonic time domain of the data stream, but need to be projected onto the often complicated geometry of directions of observation, which is essential for the interpretation of the results. Excess low-frequency (typically $\sim 1/f$) noise, for instance, is an instrumental effect that is not easily analysed when projected onto two-dimensional maps (Delabrouille, 1997).

In the following, we explore the relation between the Fourier spectrum of temperature fluctuations measured on a circle and spherical harmonic expansion coefficients on the sphere, with associated

¹MAP home page: <http://map.gsfc.nasa.gov/>

²Planck home page: <http://astro.estec.esa.nl/SA-general/Projects/Cobras/cobras.html>

³MSAM/TopHat home page: <http://cobi.gsfc.nasa.gov/msam-tophat.html>

uncertainties in the framework of gaussian statistics, and investigate how circular scans permit to analyse naturally both the signal of cosmological origin and some of the effects coming from the instrument.

2 CMB anisotropies on circular scans

2.1 Fourier spectra

The usual expansion in spherical harmonics of the statistically isotropic CMB temperature fluctuations on the sky observed with a symmetric beam reads:

$$T(\vec{n}) = \sum_{\ell=1}^{\infty} \sum_{m=-\ell}^{\ell} a_{\ell m} B_{\ell} Y_{\ell m}(\vec{n}). \quad (1)$$

Here, the coefficients $a_{\ell m}$ are assumed to be zero-mean Gaussian deviates with variances given by $\langle |a_{\ell m}|^2 \rangle = C_{\ell}$ (on assumption of statistical isotropy of the CMB temperature perturbations, here expressed via the ensemble averaging), B_{ℓ} is the beam response function (we have assumed for simplicity that the beam is symmetric), and a unit vector \vec{n} defines the position on the sphere. The functions $Y_{\ell m}(\vec{n}) = Y_{\ell m}(\theta, \phi)$ are the orthonormal spherical harmonics, defined, for $-\ell \leq m \leq \ell$, as

$$Y_{\ell m}(\theta, \phi) = \mathcal{P}_{\ell}^m(\theta) e^{im\phi}, \quad (2)$$

with

$$\begin{aligned} \mathcal{P}_{\ell}^m(\theta) &= \sqrt{\frac{2\ell+1}{4\pi} \frac{(\ell-m)!}{(\ell+m)!}} P_{\ell}^m(\cos\theta), \quad \text{for } m \geq 0, \\ &= (-1)^{|m|} \mathcal{P}_{\ell| m|}(\theta), \quad \text{for } m < 0, \end{aligned}$$

where P_{ℓ}^m are the associated Legendre polynomials. This definition of the $Y_{\ell m}$, together with the fact that the temperature is real, implies $a_{\ell m} = (-1)^m a_{\ell -m}^*$.

If only one ring of angular radius Θ on the sky is being scanned, it is convenient to use coordinates such that the observed circle is the set of points of the sphere at constant colatitude Θ . The CMB temperature on this circle, $T(\Theta, \phi)$, can be decomposed uniquely in the form of a Fourier series:

$$\alpha_m = \frac{1}{2\pi} \int_0^{2\pi} d\phi T(\Theta, \phi) e^{-im\phi} = \sum_{\ell=|m|}^{\infty} a_{\ell m} B_{\ell} \mathcal{P}_{\ell}^m(\Theta). \quad (3)$$

If $a_{\ell m}$ are uncorrelated gaussian random variables, as expected in an inflationary scenario (Bardeen et al., 1986), the same is the case also for the ring mode amplitudes α_m . The corresponding Fourier spectrum, whose components we shall denote as Γ_m , is the one dimensional analog of the C_{ℓ} spectrum on the sky. The anisotropy Fourier spectrum Γ_m is obtained from the C_{ℓ} spectrum by:

$$\langle \alpha_m \alpha_{m'}^* \rangle = \Gamma_m \delta_{mm'}, \quad (4)$$

and

$$\Gamma_m = \sum_{\ell=|m|}^{\infty} C_{\ell} B_{\ell}^2 \mathcal{P}_{\ell}^2(\Theta). \quad (5)$$

This last equation allows a straightforward computation of the ring anisotropy power spectrum Γ_m given the instrumental specifications (Θ and B_{ℓ}) and the cosmological model (C_{ℓ} spectrum as a function of the relevant parameters).

Figure 1 illustrates some properties of the ring spectrum Γ_m as compared to the usual full sky spectrum C_{ℓ} . Observational configurations chosen for the plot correspond to 1) a single ring scan of the

PLANCK satellite observing with the High Frequency Instrument (the large ring), 2) a single ring of the TopHat balloon experiment (the intermediate ring), and 3) a hypothetical small ring and a narrow beam configuration. One should note that the ring anisotropy power spectra preserve the dependence on cosmological parameters observed by the C_ℓ curves, and, if the resolution of the instrument is good enough and the ring size sufficiently large, display clearly the array of adiabatic peaks. This promotes the strategy of observing the CMB anisotropy on the rings to a very interesting status. Clearly one should be able to conduct a well guided analysis of such a data with the aid of a simple statistic, Γ_m , which, due to the natural geometric reduction from the whole sky to the circle, captures all those features of theoretical CMB anisotropy predictions — direct reflection of physical processes that perturb CMB temperature in the shape of power spectrum, and the traceable dependence on cosmological parameters — which created high level of expectations for the full sky CMB mapping missions.

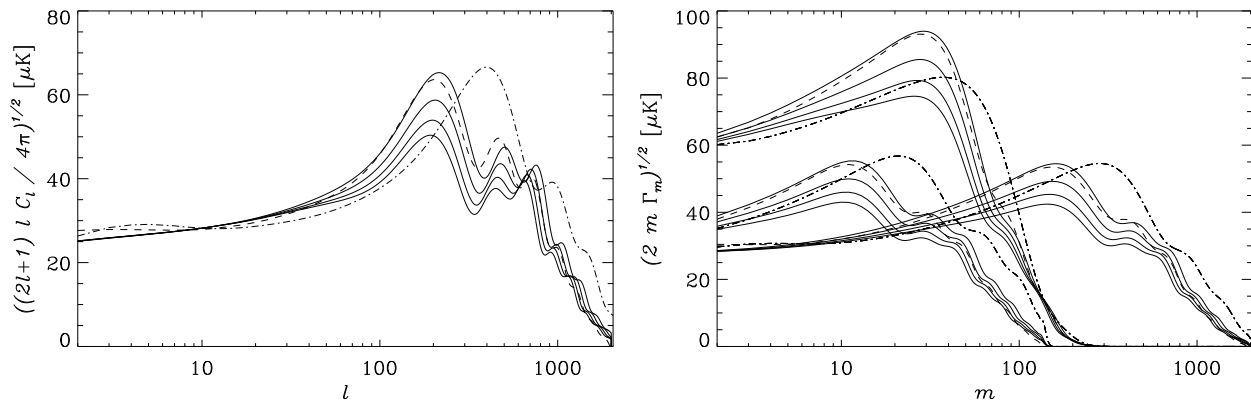


Figure 1: Left panel: Full sky power spectra C_ℓ of CMB anisotropy, smoothed with a gaussian beam of FWHM = 7 arcmin, in various Λ CDM cosmological models normalized roughly to match the CMB anisotropy detected by *COBE*-DMR. All models obey the primordial nucleosynthesis constraint $\Omega_b h^2 = 0.015$. Solid lines (top to bottom) correspond to flat, matter dominated models with Hubble constant $h = 0.5, 0.6, 0.7, 0.8$. The dashed line shows a cosmological constant dominated model with $\lambda = 0.7$ and $h = 0.8$, and the dot-dashed line shows an open model with $\Omega_0 = 0.3$ and $h = 0.65$. Right panel: One-dimensional power spectra of CMB anisotropy on circular scans computed for the same models as shown in the left panel. Three groups of curves as viewed from left to right correspond to different specifications (by the angular radius of the circle, Θ , and the FWHM of the beam) of the geometry of observations: the left group corresponds to a small ring of $\Theta = 4^\circ$, FWHM = $5'$; the middle group (amplitudes multiplied by 2 to avoid overlap with the other curves) corresponds to an intermediate size ring of $\Theta = 12^\circ$, FWHM = $20'$; finally, the right group corresponds to a large ring of $\Theta = 80^\circ$, FWHM = $7'$. Both the left and right panels show the CMB anisotropy rms amplitude per logarithmic increment of the relevant index ℓ or m , taking into account the number of degrees of freedom per mode (factors $(2\ell + 1)\ell$, and $2m$, respectively).

Ring power spectrum coefficients Γ_m can be viewed as the estimators of the spectrum C_ℓ integrated over ℓ with a certain m -dependent window function whose coefficients are simply:

$$W_\ell^{(m)} = \mathcal{P}_{\ell m}^2(\Theta) B_\ell^2. \quad (6)$$

A number of such window functions $W_\ell^{(m)}$, corresponding to the ring configurations used in Fig. 1, are displayed in Fig. 2. An important, if simple, property of these window functions, and, hence, the Γ_m coefficients, is that the power at mode m is generated by only those components of sky anisotropy for which $\ell \geq m$. This is rather important for the suborbital attempts to measure the CMB anisotropy,

which have to cope with the atmospheric effects. It has been the case for a long time that due to the variation from zenith to horizon of the length of path through the Earth's atmosphere, and the associated systematic effects in the measurements of CMB temperature, the preferred scanning strategy in CMB experiments was usually along the lines of constant elevation. Can one, in a suborbital experiment, afford to scan on any other circle than that at constant elevation? If the atmospheric temperature gradient is predominantly large-scale compared to the size of the observing ring, its contaminating effects will be confined to low- m modes of the ring anisotropy spectrum, and high- m modes will be algebraically decoupled from such a source of spurious anisotropy.

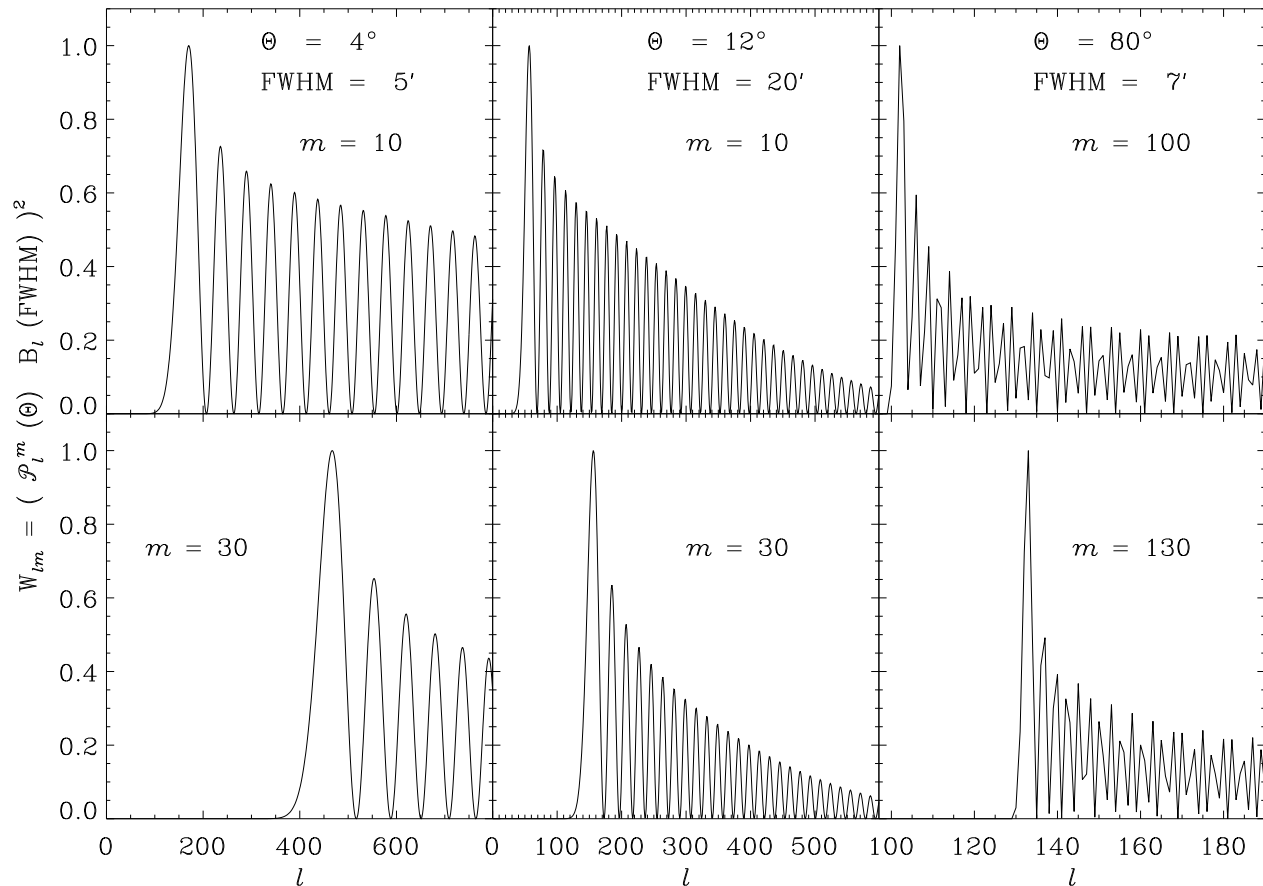


Figure 2: Window functions for computation of the CMB anisotropy ring power spectrum Γ_m , see Eqs. (5), and (6), normalised to unity at their maxima.

To what extent would a measurement of CMB anisotropy on the ring allow us to estimate the parameters of cosmological model used to describe the data? To be able to answer this question we need first to clarify the statistical properties of circular modes of CMB anisotropy, and the properties of instrumental noise as projected on the ring geometry of observations. We shall see momentarily that the estimation of uncertainties in measurements of α_m due to white noise, excess low-frequency noise, or instrumental systematic effects is simpler and more secure in the case of ring anisotropy than in the case of two dimensional maps used in C_ℓ estimation.

2.2 Statistics of Fourier transform of CMB anisotropy measurements on the rings

Here we address the issue of cosmic variance of the ring modes of the CMB anisotropy. Fourier coefficients of temperature fluctuations measured on the circle, α_m -s, are linear combinations of $a_{\ell m}$ -s, whose statistical properties they hence inherit. Specifically, Gaussian distribution of $a_{\ell m}$ -s renders

Gaussian distribution of α_m -s. Statistical isotropy of the model CMB anisotropy field results in a very special property of the m -independence of variance — $\langle |a_{\ell m}|^2 \rangle = C_\ell$, which makes the C_ℓ spectral coefficients $\chi_{(2\ell+1)}^2$ distributed. In the case of Fourier coefficients of the ring data the number of degrees of freedom associated with a specific m value is reduced to only two — $\pm m$ waves have identical variance. Hence, the cosmic variance on the Γ_m coefficients is described by the χ_2^2 probability distribution, independent of the value of m .

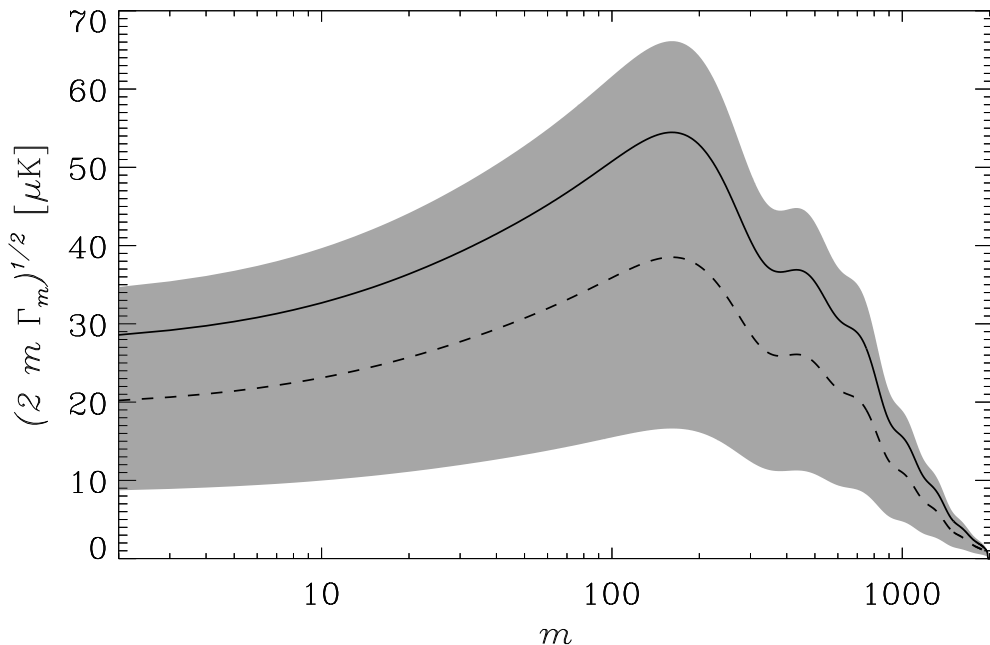


Figure 3: Statistics of the rms power of the CMB anisotropy measured on the ring. Gray band covers the 68% confidence range for each rms power coefficient and scales identically at each value of m in terms of the variance, which is shown by solid line. Dashed line shows the loci of the most probable values of the rms power, illustrating the skewness of the distribution.

In Figure 3 we illustrate the statistical properties of ring Fourier coefficients of CMB anisotropy. The plot shows a few features of probability distribution of the rms power in mode m . It is clear that the cosmic variance in the ring Fourier coefficients is large, and, unlike in the case of full sky measurements of CMB anisotropy, when available at small enough angular scales, the statistics of power at high m do not improve compared to those in low- m modes, as the ring configuration allows just two degrees of freedom per mode, independent of m . It is clear that the only opportunity for improvement of statistics of the measurements of ring modes of CMB anisotropy rests with repeating the observations on many rings. The essential issues of assessing the ring to ring covariance of the Fourier modes of CMB anisotropy will be addressed in detail in a separate paper (Górski, Delabrouille, and Hivon, in preparation).

3 Noise on circular scans

Now we turn to the estimation of the projection of instrumental noise onto a ring of data. Noise, unlike the CMB temperature anisotropies, is a time-dependent process which is independent (to first order) of the position on the sky. The same is true of many instrumental effects in the measured signal (system impulse response, sampling,...), but we first limit our discussion to a simple Gaussian noise

as an illustration of the connection between the measured data stream and the signal reprojected on the ring.

Let us assume that data is collected by a total-power experiment as PLANCK, TopHat, BEAST or DIABOLO, and that a circle on the sky is scanned continuously N times, with a spinning frequency f_{spin} (spinning period T_{spin}). The output of each detector is a signal $s(t)$, whose value as a function of time can be written as:

$$s(t) = u(\phi(t)) + n(t). \quad (7)$$

In this equation, $\phi(t) = 2\pi f_{\text{spin}}t$ is the longitude angle on the circle. The way it depends upon time reflects the scanning strategy. $u(\phi) = T(\Theta, \phi)$ is the useful signal from the sky, i. e. the temperature anisotropy smoothed with the beam. It is a 2π -periodic function of ϕ for fixed Θ . If anisotropies are correctly represented by a gaussian random field, the Fourier components u_m of the Fourier series decomposition of $u(\phi)$ are realisations of the random variables α_m defined in the previous section. The noise $n(t)$ is assumed to be a realisation of a Gaussian stationary random process with zero mean and a bilateral spectrum $\mathcal{S}_n(f)$ which, over a large range of frequencies, can be typically of the form:

$$\mathcal{S}_n(f) = a \left(1 + \left(\frac{f_{\text{knee}}}{|f|} \right) \right) \quad (8)$$

This is the simple case of the so-called $1/f$ noise.

Given the signal timeline as defined in Eq. (7), the estimation of the Fourier components of anisotropy on the ring can be done by computing the integral:

$$\begin{aligned} s_m &= \frac{1}{NT_{\text{spin}}} \int_0^{NT_{\text{spin}}} s(t) \exp\left(-\frac{2i\pi mt}{T_{\text{spin}}}\right) dt \\ &= u_m + \frac{1}{NT_{\text{spin}}} \int_0^{NT_{\text{spin}}} n(t) \exp\left(-\frac{2i\pi mt}{T_{\text{spin}}}\right) dt. \end{aligned} \quad (9)$$

Under the present hypotheses (no foregrounds, uncorrelated gaussian noise), this quantity s_m is an unbiased estimator of α_m , which variance originates in only two sources of uncertainty. First, there is the theoretical ‘‘cosmic’’ or ‘‘sample’’ variance due to the fact that u_m is just one realisation of α_m , as discussed in paragraph 2.2. Second, there is the uncertainty due to the detection process (i. e. due to the noise $n(t)$). Let us denote as n_m the quantity

$$n_m = \frac{1}{NT_{\text{spin}}} \int_0^{NT_{\text{spin}}} n(t) \exp\left(-\frac{2i\pi mt}{T_{\text{spin}}}\right) dt. \quad (10)$$

Each of the n_m -s can be viewed as a realisation of a gaussian random variable. They obey the correlation statistics:

$$\langle n_m n_{m'}^* \rangle = \int_{-\infty}^{\infty} \mathcal{S}_n(f) H_m(f) H_{m'}^*(f) df \quad (11)$$

where $H_m(f)$ is given by:

$$H_m(f) = e^{(i\pi N(f/f_{\text{spin}} - m))} \times \frac{\sin(\pi N(f/f_{\text{spin}} - m))}{\pi N(f/f_{\text{spin}} - m)}. \quad (12)$$

Interestingly, but not surprisingly, there may be some correlations between Fourier amplitudes of the noise reprojected on the ring, depending on the nature of the noise spectrum $\mathcal{S}_n(f)$. However, if the number N of scans on a circle is large and the noise spectrum \mathcal{S}_n is not too steep ($1/f$ is fine), the expectation value of $n_m n_m^*$ becomes:

$$\langle n_m n_{m'}^* \rangle \simeq \frac{\mathcal{S}_n(m f_{\text{spin}})}{NT_{\text{spin}}} \delta_{mm'}. \quad (13)$$

Thus, for each individual m value, the uncertainty in $s_m s_m^*$ induced by noise depends on f_{spin} through the noise spectrum value $\mathcal{S}_n(m f_{\text{spin}})$, and upon the total integration time NT_{spin} . For a given experiment, the spinning frequency and total integration time should be optimised by comparing the level of the noise spectrum to the expected spectrum of the signal of astrophysical origin. Usually, the noise spectrum decreases with increasing f , and thus the minimisation of $n_m n_m^*$ requires to spin fast, up to a compromise which depends on other experimental considerations.

If the number of scans on a circle, N , is large, and the noise spectrum \mathcal{S}_n is not too steep, the expectation value of $s_m s_m^*$ averaged over sky realisations of the CMB *and* noise realisations is:

$$\langle s_{m'} s_m^* \rangle \simeq \left(\Gamma_m + \frac{\mathcal{S}_n(m f_{\text{spin}})}{NT_{\text{spin}}} \right) \delta_{mm'}. \quad (14)$$

Thus a direct comparison of the signal and noise spectra for typical next-generation experiments is quite straightforward in the ring formalism and is presented here in Fig. 4.

In the top panel of Figure 4, we have plotted together the rms values of Γ_m for three different experiments and two different cosmological models, and the noise-induced sensitivity limits to individual Γ_m components. Experimental parameters chosen for the plot are representative of the next generation balloon-borne or satellite experiments. The pure white noise contribution, proportional to $m^{1/2}$, has the shape of an exponential because of the logarithmic scale for m . $1/f$ noise alone would appear on the plot as an horizontal line, with amplitude equal to that of the white noise at $m = m_{\text{knee}} = f_{\text{knee}}/f_{\text{spin}}$. As long as m_{knee} is smaller than a few, the excess $1/f$ noise induces a slight flattening of the noise curve for low m , with negligible total additional noise power.

4 Other systematics and instrumental effects

Apart from noise, there are a few effects of instrumental origin which can be understood much easier on timelines than on maps of the sky. Some of these effects can be described as those of filters with a known impulse response, $h(t)$. The Fourier transform of the impulse response, $H(f)$, is known in signal processing as the transfer function of the filter. For such filters, the filtering theorem states that if a signal $u(t)$ has a spectrum $\mathcal{S}_u(t)$, the corresponding filtered signal, $u_F(t) = u(t) \star h(t)$, has spectrum $\mathcal{S}_u(t)|H(f)|^2$. Two important instrumental effects can be addressed with this formalism.

4.1 Time constant of bolometers

A typical bolometer for CMB anisotropy observations is a temperature-sensitive resistor heated by incoming radiation and cooled by a heat-conducting connection to a sub-kelvin thermal bath. The response of such a system to an impulse of incident power is:

$$h(t) = \frac{1}{\tau} \exp(-t/\tau) \quad (15)$$

The constant τ is known as the time constant of the bolometer. It is set by physical characteristics of the bolometer ($\tau = C/G$, where C is the heat capacity of the bolometer and G the effective conductivity of the link to the thermal bath). However, other bolometer characteristics, and in particular the sensitivity of the bolometer, depend on the same parameters. Thus, it is crucial, for bolometer optimisation, to understand the effect of the time constant of the bolometers on the spectrum of the useful astrophysical (and especially cosmological) signal.

The transfer function $H(f)$ corresponding to the impulse response of equation 15 is:

$$H(f) = \frac{1}{1 + 2i\pi f\tau} \quad (16)$$

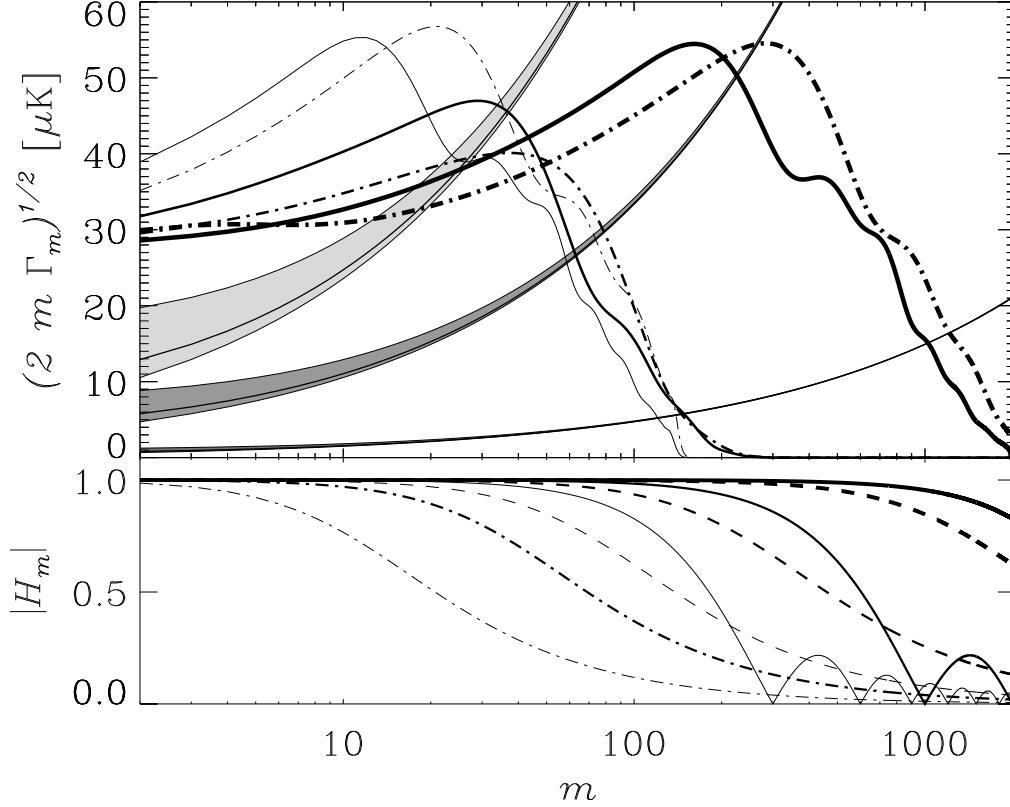


Figure 4: Top panel: Power spectra Γ_m of signal and noise for the following set-ups of CMB anisotropy measurements: 1) the ring radius of $\Theta = 4^\circ$ and FWHM = 5 arcmin — light lines, 2) $\Theta = 12^\circ$ and FWHM = 20 arcmin — medium-width lines, and 3) $\Theta = 80^\circ$ and FWHM = 7 arcmin — heavy lines. Solid lines show the predictions of standard CDM model, and dot-dashed lines those of an $\Omega_0 = 0.3$ open model, both normalized to *COBE*-DMR. Three gray bands show the range of rms values of instrumental noise contributions. Bottom edges of the gray bands correspond to pure white noise behaviour of the detector. Solid lines inside the bands illustrate the noise enhancement due to the $1/f$ component when the knee frequency is equal to the spin frequency on the ring scan. The upper edges of the gray bands correspond to $f_{\text{knee}}/f_{\text{spin}} = 5$ (excess low frequency noise grows with $f_{\text{knee}}/f_{\text{spin}}$). The assumed (white noise) detector performance is characterized by sensitivity of $1 \text{ mK}\sqrt{s}$ and total integration time of 20 and 100 hours for the upper two bands (light and medium gray respectively), while the third, narrow, dark gray noise band corresponds to a sensitivity of $20 \mu\text{K}\sqrt{s}$ and integration time of 2 hrs. Bottom panel: Illustration of the effects of sampling and bolometer time constant (see text). Heavy lines correspond to spin period of 1 min, and illustrate the effect of sampling at 10 ms — solid line, and bolometer time constant of 6 ms — dashed line. Medium-width and light curves correspond to spin period of 10 s, and 3 s, respectively. For these two spin rates the solid lines illustrate the effect of sampling at 10 ms, and the dashed and dot-dashed lines show the effect of bolometer time constant of 6 ms, and 40 ms, respectively.

Using the relation between m and frequencies of the signal, $m = f/f_{\text{spin}}$, the attenuation function A_m on the Γ_m corresponding to the effect of the time constant of the bolometers is:

$$A_m = |H_m|^2 = \frac{1}{1 + (2\pi f_{\text{spin}}\tau)^2 m^2} \quad (17)$$

and instead of measuring the quantities Γ_m , the instrument measures $A_m\Gamma_m$.

4.2 Effect of the sampling frequency

Another instrumental parameter which needs to be set carefully by designers of CMB experiments is the sampling frequency. It should be high enough in order to avoid aliasing, but making it unnecessarily high results in a very large set of data, with the associated problems of data storage and telemetry, especially for satellite or long duration ballooning experiments.

Again, the effect of the sampling rate can be understood very simply as that of a filter. If sampling is modelled by a perfect integrator over a period T_0 (which is the inverse of the sampling rate) for obtaining each sample, the corresponding impulse response is:

$$h(t) = \frac{1}{T_0} \text{rect}(T_0), \quad (18)$$

where $\text{rect}(T_0)$ is the function whose value is 1 between $t - T_0/2$ and $t + T_0/2$, and 0 elsewhere. The corresponding transfer function is

$$H(f) = \frac{\sin(\pi f T_0)}{\pi f T_0} \quad (19)$$

and the corresponding attenuation function A_m on the Γ_m is:

$$A_m = |H_m|^2 = \frac{\sin^2(\pi m f_{\text{spin}} T_0)}{(\pi m f_{\text{spin}} T_0)^2} \quad (20)$$

Attenuation functions for these two effects are plotted in the bottom panel of Figure 4.

5 Conclusion

In this paper, we presented the formalism to project the CMB anisotropy predictions and instrumental noise effects on the rings of data. Because of the feasibility of experimental setup for CMB observations with circular scans, and simplicity of the data analysis on such scans, we believe that collecting CMB anisotropy data in this format is an interesting option for the next generation of anisotropy experiments. It provides a natural frame for studying the statistics of CMB anisotropies, in which many instrumental effects can be modelled and analysed under the most natural connection between the time stream of data and the spatial distribution of the directions of measurements. We attempted to illustrate this point comprehensively in our Figure 4. Given that this comparative plot allows to present simultaneously a natural rendition of a number of factors that affect the attempts to measure the CMB anisotropy on the celestial rings, we believe that Fig. 4 should provide significant insights on optimization of experimental setup for future CMB experiments.

For the most ambitious CMB programmes such as PLANCK, many such scans will have to be merged into two-dimensional maps. The circular scan method described in this paper is a useful intermediate step in the analysis of such data in the global analysis of CMB anisotropies on the celestial sphere.

Acknowledgments

Original inspiration for KMG to consider the circular scanning came from discussions of the UCSB HACME experiment with P. Lubin and M. Seiffert, whereas JD's interest in the subject was stimulated by discussions with François-Xavier Désert and Jean-Loup Puget over the choice of an optimal scanning strategy for the DIABOLO 1997 observations. JD would like to thank Eric Aubourg, Nathalie Palanque-Delabrouille and Simon Prunet for help and suggestions in numerical computations of Γ_m 's for the first draft of this paper. CMB anisotropy power spectra in the flat CDM models were computed using the code CMBFAST (Seljak & Zaldarriaga, 1996). JD was supported by a PhD research grant from CNES, the French national space agency. KMG and EH were supported in part by the Danish Research Foundation through its establishment of the Theoretical Astrophysics Center.

References

- [1] Bardeen, J.M., et al. , 1986, ApJ, 304, 15
- [2] Bersanelli et al. , 1996, COBRAS/SAMBA : Report on the Phase A Study
- [3] Delabrouille, J., 1997, to be published in A&A supplement series
- [4] Seljak, U. & Zaldarriaga, M., 1996, ApJ, 469, 437